Journal of Advanced Research in Applied Sciences and Engineering Technology

Journal homepage:
https://semarakilmu.com.my/journals/index.php/applied_sciences_eng_tech/index
ISSN: 2462-1943

Resistance Evaluation for the Submerged Glider System using CFD Modelling

Alaaeldeen Mohamed Elhadad Ahmed[1,*]

[1] Shipbuilding Engineering Department, Military Technical College, Cairo, Egypt

ARTICLE INFO

Article history:
Received 8 December 2022
Received in revised form 30 December 2022
Accepted 23 January 2023
Available online 13 February 2023

Keywords:
Submerged glider system; Resistance; NACA flapping wing; CFD

ABSTRACT

The underwater gliders are type of autonomous underwater vehicles, which are in their way to be used instead of traditional propellers or thrusters. They are used as submerged gliders or as a part connected to floating hull which is propelled by it. The underwater system depends on different number of hydrofoils (underwater wings) that allow it to glide forward while descending through the water. This paper concentrates on three critical design details: profile of the wings, multiple flapping wings and their angle of attack (AoA), and a method is focused on the mesh generation to predict calm water resistance for the submerged glider system while considering the profile and the maximum rotating angle of the wings and rudder. Flow around submerged wing system model has been calculated at different Froude numbers ranging from 0.1 to 0.6. The grid generator is established for meshing the computational domain with structured hexahedral and unstructured tetrahedral grid. Simulations are carried out using commercial CFD code ANSYS Fluent 19 to calculate calm water resistance of the submerged glider system with different number of hydrofoils. The results conclude that the cambered plate was chosen to design the rudder at 19° AOA and the hydrofoil NACA0012 can be practically applied in the design of the wings at 15° AOA from the resistance point of view. In addition, this investigation introduces a new application for CFD calculations in estimating the resistance of the submerged glider system.

1. Introduction

Wave glider (WG) as long-duration ocean robot is a new approach for achieving wide range of missions and applications including defence, maritime security and environmental investigations for marine science missions as shown in Figure 1 [1]. It can be programmed for being a station for certain time or to make a trip along definite waterway to replace many buoys and AUVs for a variety of applications [2]. One benefit of this novel platform over moored buoys is that users can regulate in real time the glider's placement in extremely hazardous conditions far from the coast. The on-board weather station on the WG is built to function properly on a moving platform in rough seas. The submerged wings mechanically convert ocean wave energy into thrust and work as a tug to pull the surface float. The glider frame includes the submerged wings and attached rudder.

* *Corresponding author.*
E-mail address: dr.aladdinahmed@gmail.com

https://doi.org/10.37934/araset.29.3.147159

Mathematical modelling using computational fluid dynamics (CFD) for quantitative prediction of fluid flow has become trending approach for designing and optimization of marine vessels [3] . Our study is focused on CFD approach in solving the fluid flow of the submerged wing system to overcome the shortage of design data and introducing a method to evaluate calm water resistance around the wings of glider system [4]. This is significant for modifying the submerged glider system using CFD simulation techniques to increase the mission capabilities and durability [5].

Fig. 1. The submerged glider system (glider, wings and rudder) (www.bing.com/images)

The marine creatures' tails and fins are designed to provide thrust and lift force so they may move ahead or manoeuvre with ease. For the underwater system's propulsion system, a flapping foil has been used. In this study, we simulate the passive foil flapping that occurs; while a floater rides a wave and is affected by the heaving action of the floater.

The single foil NACA-0012 which selected as the best choice of the hydrofoil as compared to the other hydrofoil sections is utilized to flap at a certain position of angle of attack. Secondly is the prediction of the thrust force of the flapping foil of the NACA-0012 at different location of the rotation axis of the foil.

It is well acknowledged that no one model can accurately predict all of the properties of fluid flow and its interactions with airfoils while consuming only a modest amount of processing power. As more physical phenomena are taken into account, including turbulent, compressible, and multiphase flows, among other pertinent circumstances, the modelling problem becomes increasingly difficult. Numerous numerical simulations and experimental studies have been carried out to evaluate the aerodynamic coefficients and boundary layer properties. Previous studies have demonstrated that the Reynolds number and angles of incidence have a significant impact on the aerodynamic performance of 2-D airfoils.

In this paper, a study of hydrodynamic characteristics was conducted by CFD simulation using the k-ω SST model [5]. The lift and drag coefficient as well as pressure and velocity variation on the surface of the submerged glider with 16 fins of NACA 0012 at different angle of attack is studied for a different Reynolds number. Important hydrodynamic parameters are identified, such as the maximum lift and the maximum effective angle of attack. In order to get a trustworthy conclusion, existing methods for studying the hydrodynamic properties of hydrofoils through experiments were contrasted. The simulation was expanded to include higher attack angles that went beyond the stall angle. This research examined the turbulence model's reliability analysis.

2. Submerged System Model

The model is composed of longitudinal rigid bar with fins system which rotates with angle of attack (AOA) about the axis [6]. This fins system has different number of identical laminar fins (12 fins and 16 fins divided evenly on both sides) and the longitudinal profiles of the 3D models prepared for CFD calculations are shown in Figure 2 and Figure 3 respectively. The float is connected to fins system

with a tether which contains devices that detect and correct twisting in addition to a rudder for sailing.

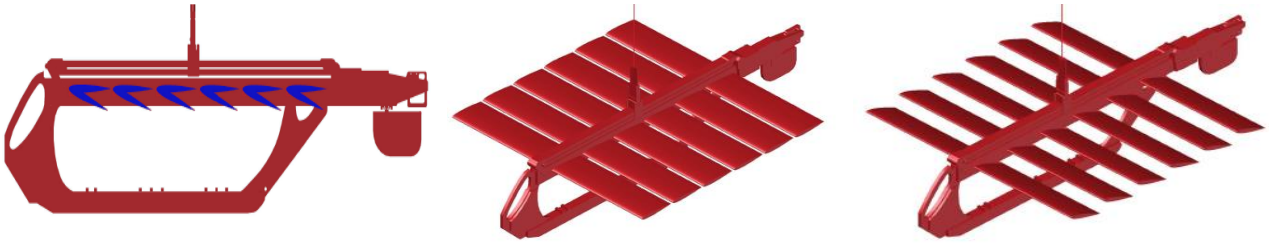

Fig. 2. Geometry and the 3D model of the submerged wing system (12 fins) at 0° and AOA

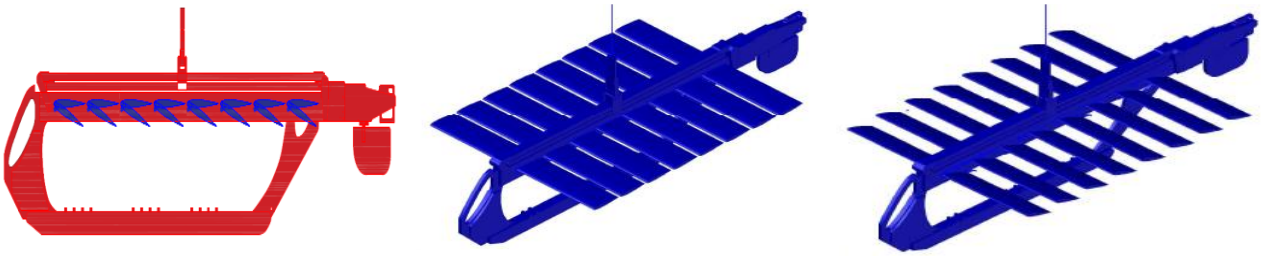

Fig. 3. Geometry and the 3D model of the submerged wing system (16 fins) at 0° and AOA

Javafoil software was applied to evaluate the hydrodynamic characteristics of the submerged part and analyse pressure distributions, lift and drag forces for the fins and the rudder [7, 8] as illustrated in Figure 4. Specifications of the wing system models tested are presented in Table 1.

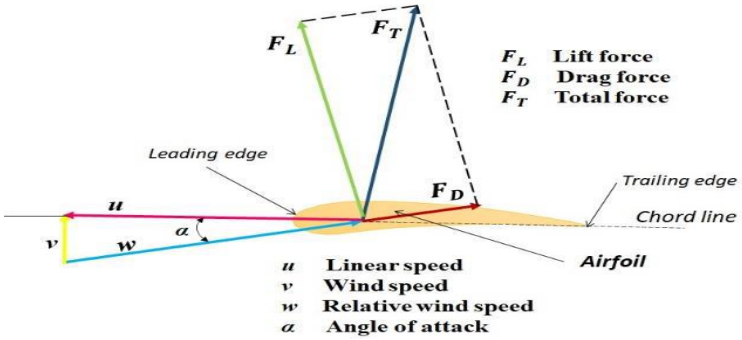

Fig. 4. Angle of attack and relative foil speed and forces

Table 1
Specifications of the submerged wing system

Description	Units	12 fins Dimensions	16 fins Dimensions
Length (L) x Height (h)	m	1.90 x 0.42	2.45 x 0.45
Width (b)	m	1.15	1.25
Underwater depth (l)	m	7.00	6.20
Water Density	$Kg.sec^2/m^4$	101.93	101.93
Kinematic Viscosity	m^2 /sec	$1.28*10^{-6}$	$1.28*10^{-6}$

3. Rudder and Wing Pattern

The simple geometrical mathematically defined cambered plate presented an appropriate selection for the rudder of the submerged system to configure the realistic suggested model as demonstrated in Figures 5 [9, 10].

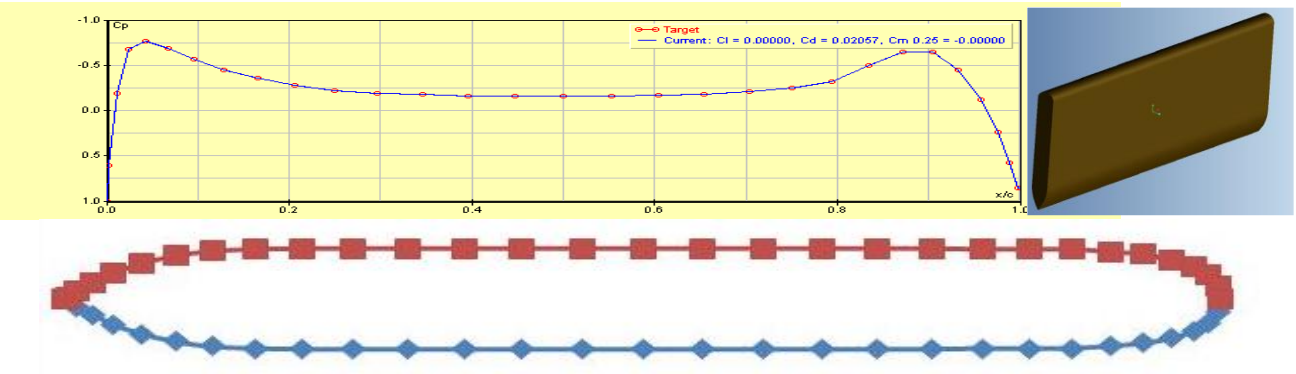

Fig. 5. Cambered plate profile

As previous work for the submerged part of wave glider for rudder design, Figure 6 shows the flow field of compared plate at Rn 4x10^4 and 20^o AoA. Cambered plate was chosen to design the rudder at 19^o AOA as shown in Figure 7. Table 2 and Figure 8 entails the forces acting on the cambered plate at several angles of attack at defined Reynolds number [11] . Thus, numerous airfoil designs have been analysed at a wide range of operating conditions is the Reynolds number for different hydrodynamic performances. One of the challenging design and hydrodynamic analysis of airfoils is at low Reynolds numbers.

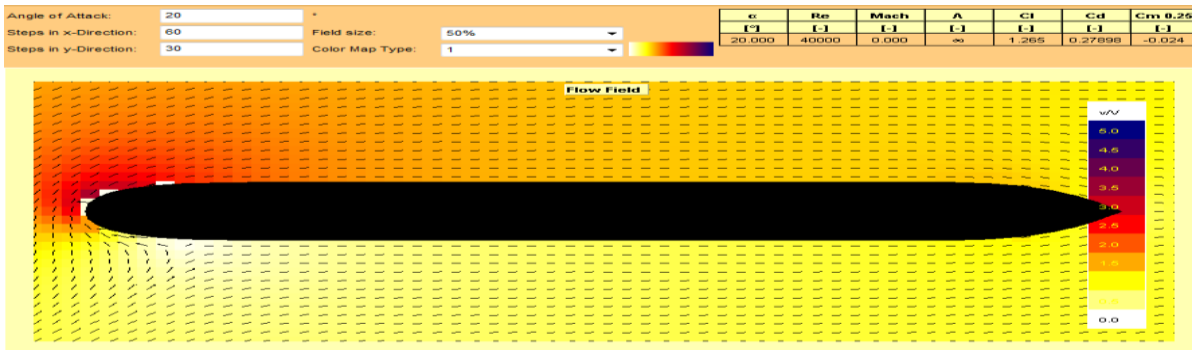

Fig. 6. Rudder flow field at 20^o AoA

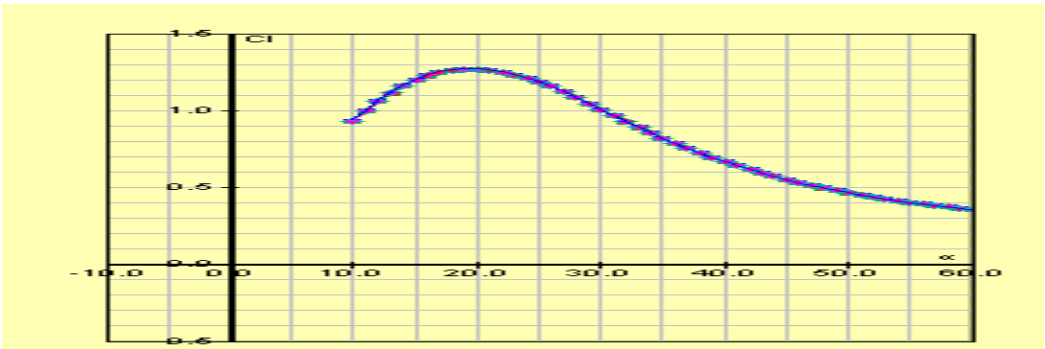

Fig. 7. Rudder angle of attack

Table 2
Rudder calculations

Angle of attack	Lift coefficient	Drag coefficient	Lift force [N]	Drag force [N]
10	0.93	0.08	30.84	2.75
15	1.21	0.16	35.61	5.02
19	1.27	0.23	42.06	7.63
25	1.19	0.41	39.37	13.45

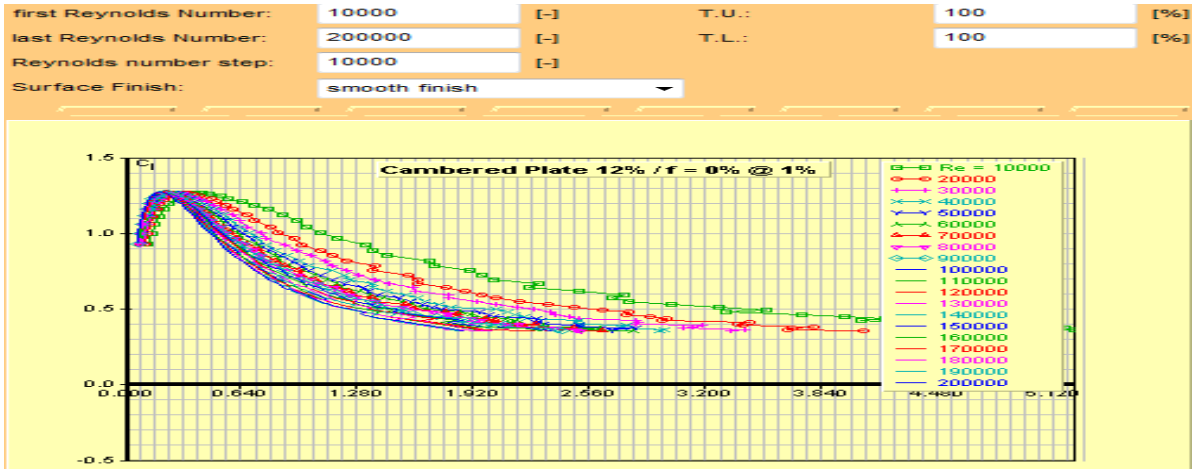

Fig. 8. Cambered plate Cl values at different Rn

The simple geometrical mathematically defined NACA 0012 foil presented an appropriate selection for the fins of the submerged system to configure the realistic suggested model as demonstrated in figure 9 [9, 10]. The NACA 0012, a well-researched airfoil from the 4-digit series of NACA airfoils, was employed in this study. The NACA 0012 foil is symmetrical and without camber, as indicated by the 00. The number 12 denotes that the chord length and thickness of the foil are 12% the same. In order to confirm the current simulation, Reynolds numbers for the simulations range from Re=0.6x10^5 to Re=0.2x10^6, matching the trustworthy experimental data from NACA (1959).

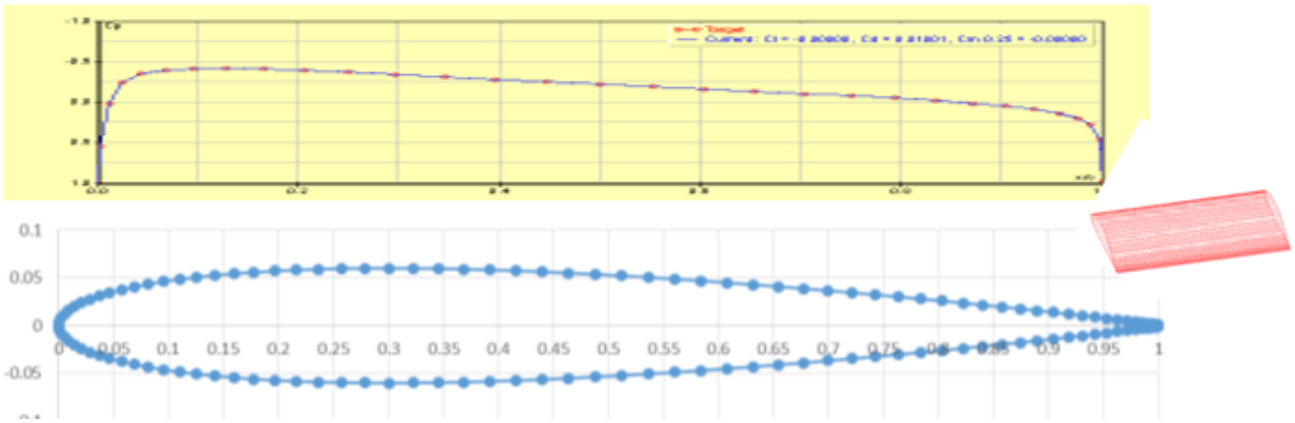

Fig. 9. NACA0012 foil profile

According to the previous work by using javafoil software; comparison between different airfoils to select the appropriate foil used as wings for the submerged glider was done. NACA 0012 was chosen as a hydrofoil section for subsurface wing system according to the results of AoA, lift and drag coefficients [12, 13]. In our work, Lift coefficient Cl calculated at different AoA from 10 ° to 22° with increment 1° at deferent Rn. It has maximum lift and drag coefficients of 1.02 and 0.15 at AOA of 15° at different Reynolds numbers as shown in figures 10a and 10b respectively.

As the angle of attack is increased, the separation flow region continues moving towards the leading edge. At certain critical AoA at 15°, the lift coefficient will drop rapidly and drag coefficient will increase rapidly. The essential AoA for this situation is known as the stall angle. The hydrofoil will have its highest lift coefficient at the stall angle.

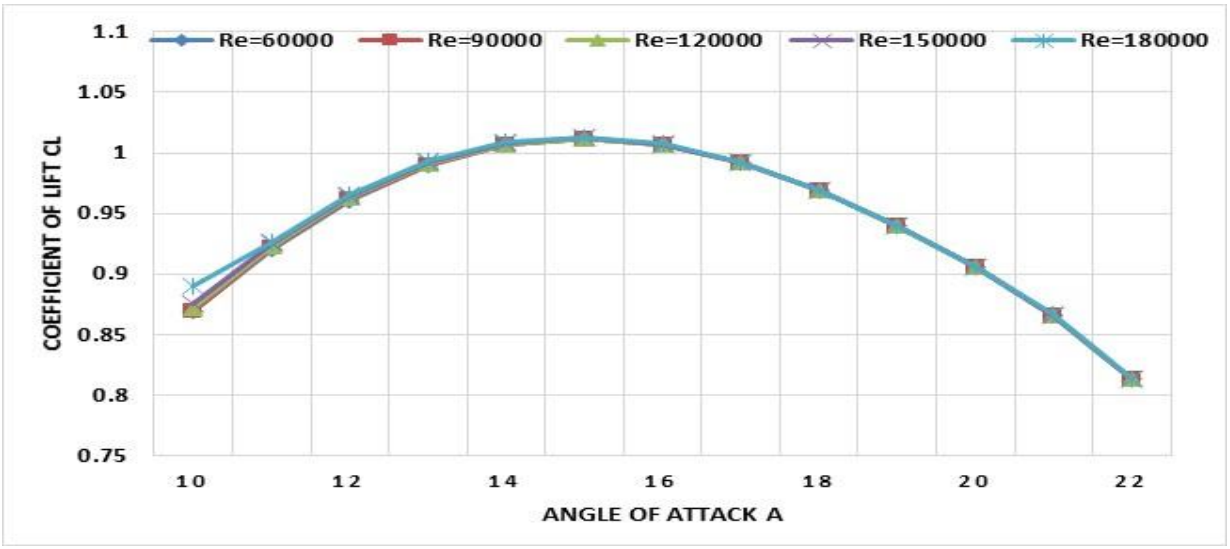

(a)

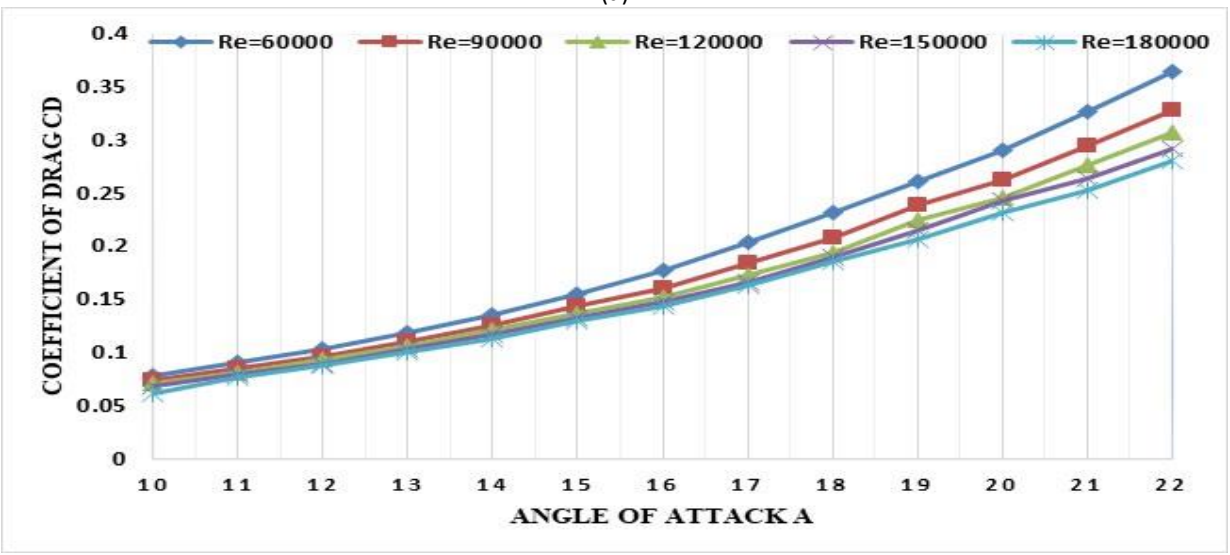

(b)

Fig. 10. Coefficient of lift (a) and drag (b) for hydrofoil NACA0012 at different Reynolds numbers

Table 3 shows the forces acting on the NACA 0012 at several angles of attack at the defined Reynolds number[14, 15]. The flow field shown in Figure 11 expresses the flow around the hydrofoil at 15° AoA at Rn 0.1 x 10^6. The hydrofoil's surface was all that the panel analysis method could analyse, but once the surface velocity was known, the potential flow theory could be used to calculate the flow velocity and direction, as shown in Figure 12. Each grid point is evaluated after the surface velocity distribution has been solved for [16, 17].

Table 3
Results for lift and drag force for NACA 0012 hydrofoil

Angle of attack	Lift coefficient	Drag coefficient	Lift force [N]	Drag force [N]
10	0.87	0.08	41.40	3.75
15	1.02	0.15	48.21	7.42
18	0.96	0.22	45.23	11.02
20	0.91	0.29	43.17	13.85

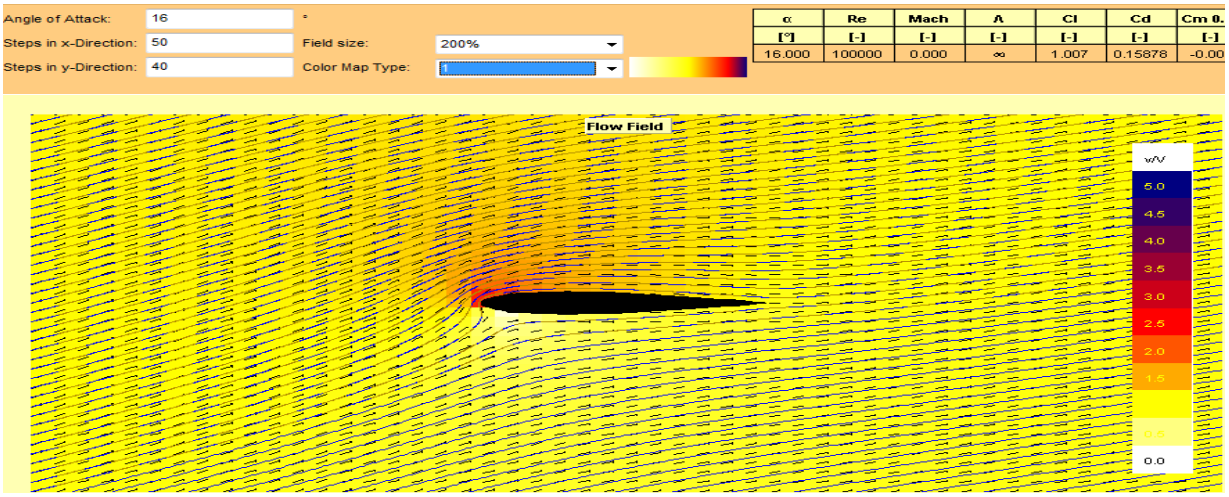

Fig. 11. NACA 0012 flow field at 15° AoA at Rn 0.1 x 10^6 for velocity ratio

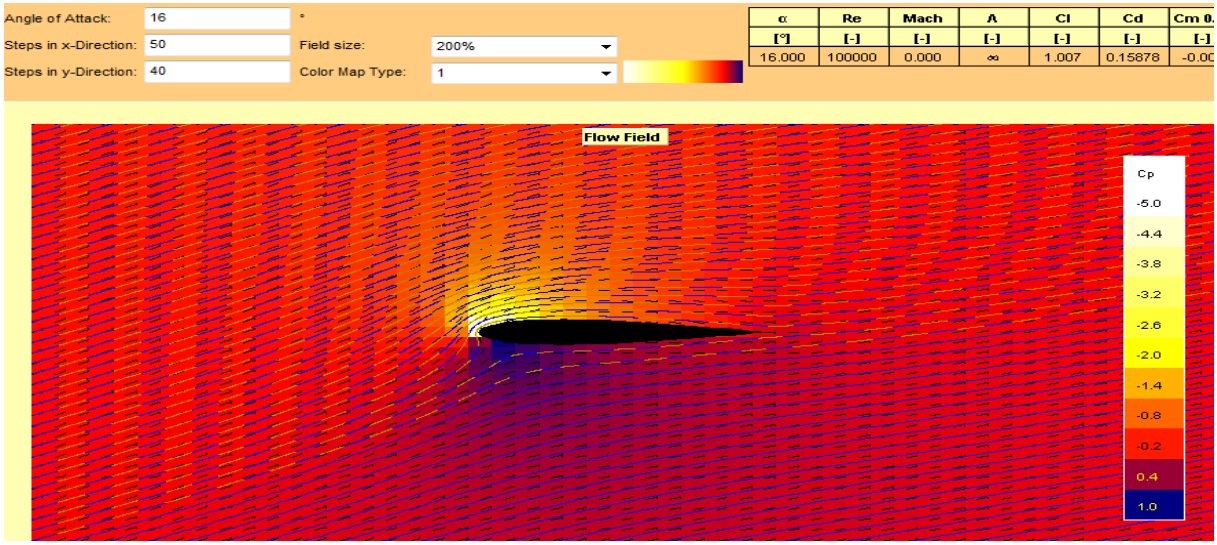

Fig. 12. Streamlines around the NACA 0012 for pressure coefficient

4. Computational Domain and Grid Generation

The 3D model geometry was created in CAD then imported to grid generator GAMBIT for meshing the model and its domain. The control volume was chosen to be cylindrical shape around the model and the whole domain was cubical shape subdivided into sub volumes to create structured multi-block grid. Unstructured and structured hybrid mesh pattern were created for model domain and remaining domain respectively as illustrated in Figures 13 and 14. As is displayed in these figures, the Tri-Pave face mesh are generated in both cases and the mesh density of the separate models should be equal to each other to make sure the comparability of simulation data.

This mesh presented flexibility in choice of the mesh elements types around the model regarding the complexity of the system geometry [18]. Finally, boundary types are specified and mesh files are exported. Now it is well prepared for simulation calculation in FLUENT software.

The Cartesian coordinate system was setup with x-axis pointing towards the bow, y-axis upwards and z-axis to portside [19]. The domain inlet boundary was at a distance of 1 L_{model} forward of the wing system while the outlet boundary was located 3 L_{model} aft of the model. The domain height was 1.5 L_{model} with extra depth equal to the tether length and its width was 2 L_{model} [20]. Three different mesh sizes were evaluated in our study for the 16 wing-system model. The number of elements in

coarse, medium and fine mesh grid were 723,220, 858,620 and 974,487 respectively. The CFD solution provided geometry creation of the model with computational grid generation, analysis of the problem and post processing of the results [21]. The resolution of the mesh was more magnificent, close to the airfoil boundary layer regions where greater computational accuracy was needed.

A typical situation at sea is sea state condition 3-4, which has an average period of 4.6 seconds and a significant wave height of 1.4 metres. Because seawater has a vertical mean velocity of roughly 0.6 m/s, the vertical velocities employed in this paper—ranging from 0.1 m/s to 0.6 m/s—can successfully show how the performance curves' changing trends have changed over time.

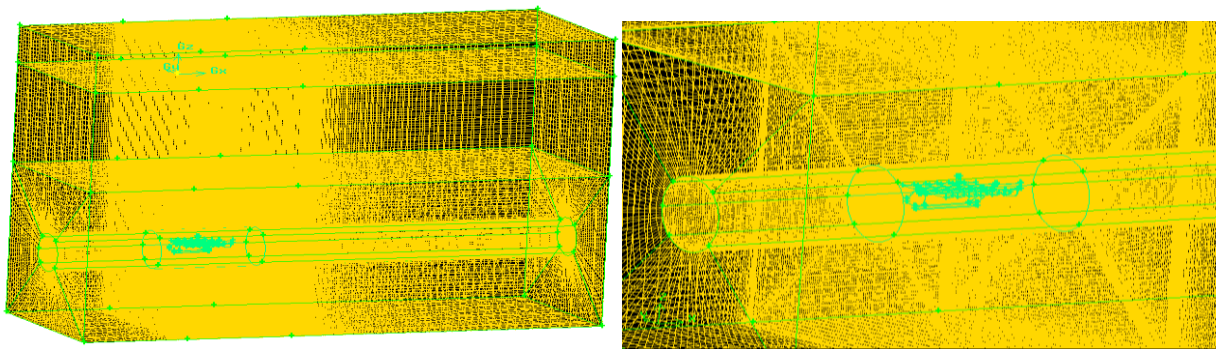

Fig. 13. Mesh of computational domain in gambit

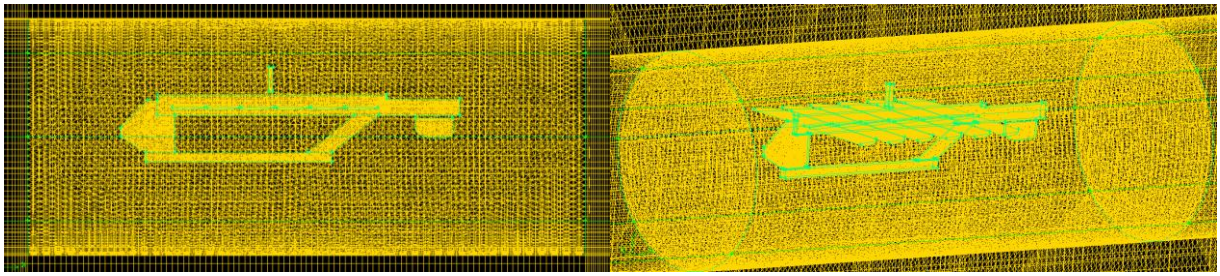

Fig. 14. Close-up view of the hybrid unstructured mesh

5. Boundary Conditions and Convergence Criteria

Our study used ANSYS Fluent 19 software for resistance prediction. The boundary conditions used for the system domain were velocity inlet and outflow for the inflow (air and water) and outflow surfaces respectively, whereas the flow speed was equivalent to the model speed. The domain bottom, top and sides were non-slip condition take into account the gravity effects on boundary conditions. The characteristics of any cell either one phase or mixture between two phases depend on the value of volume fraction [22]. Calculations were done for angle of attack ranging 18°.

The turbulence model studied in the suggested wing system was shear-stress transport (SST) k−ω turbulence model in order to approach RANS equations where three-dimensional unsteady, two-phase (air and water) and viscous turbulent flow field were examined. SST k-ω model developed by Menter is stated as follows [23]:

$$\frac{\partial}{\partial t}(\rho k) + \frac{\partial}{\partial x_i}(\rho k u_i) = \frac{\partial}{\partial x_j}\left(\Gamma_k \frac{\partial k}{\partial x_j}\right) + G_k - Y_k + S_k \quad (1)$$

$$\frac{\partial}{\partial t}(\rho \omega) + \frac{\partial}{\partial x_i}(\rho \omega u_i) = \frac{\partial}{\partial x_j}\left(\Gamma_\omega \frac{\partial \omega}{\partial x_j}\right) + G_\omega - Y_\omega + D_\omega + S_\omega \quad (2)$$

where; G_k *and* G_ω represent the generation of turbulence kinetic energy due to mean velocity gradients, and the generation of ω. Γ_k and $\Gamma_\omega$represent the effective diffusivity of k and ω respectively. Y_k and Y_ω represent the dissipation of k and ω due to turbulence. D_ω represent the cross-diffusion term, S_k and S_ω are user-defined source terms.

A numerical method for solving multiphase free-surface flow was the Volume of fluid (VOF). A straightforward procedure (semi-implicit methods for pressure-linked equation) was used to pair the pressure and velocity fields [24]. By keeping track of the residuals of continuity, velocity, turbulence, volume fraction, and drag force, the assessment of solution convergence was calculated. It was assumed that the residual convergence value would be $1e^{-07}$[25].

6. CFD Results and Discussions

The total resistance of the 12 fins system model was calculated by calculating the total resistance for the submerged glider for the three different grids. The calculations were carried out for Froude number ranging from 0.10 to 0.40 as illustrated in Figure 15. The three grid results were in relative compliance. The numerical results were compared to experimental results for fabricated model tested in Harbin engineering university towing tank. The difference of the predicted resistance was limited with equal order of magnitude. This means the linear free-surface boundary conditions has described well the flow for this model. The compared results are accepted from resistance point of view.

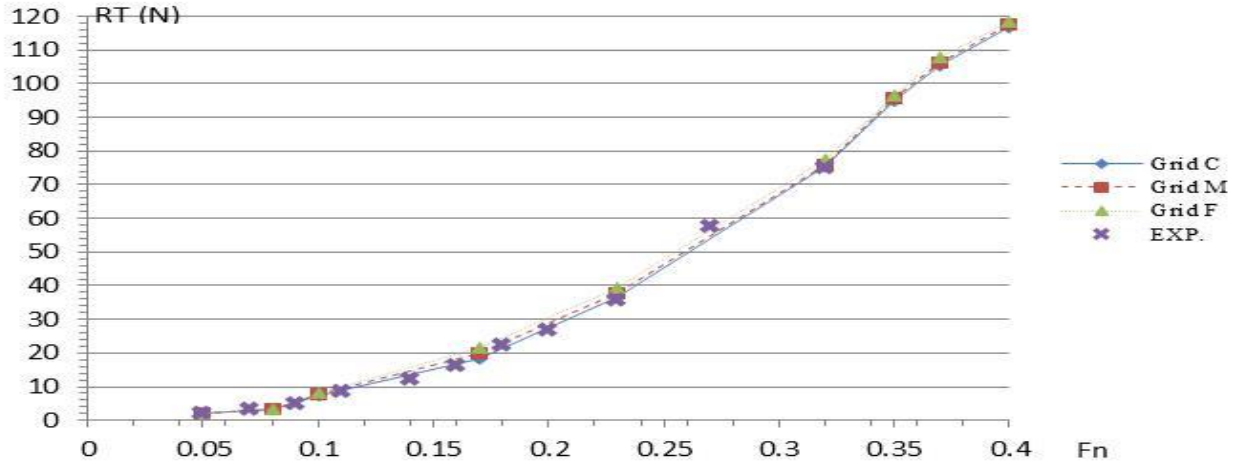

Fig. 15. Calm water resistance curves for the model using CFD

The method used for the total resistance calculation of the 16 fins system model, which was calculated for the three grids. The calculations were carried out for ten Froude numbers ranging from 0.10 to 0.60 at 15° AOA. The overall grid elements of domain for the 16 fins-model were 805, 645 998,735 and 1,154,532 hexahedral cells. The calculated drag on the model was recorded every 200 iterations, in order to judge the convergence of the solution as demonstrated in Figure 16. The three grid results agreed with each other. The anticipated resistance difference was also controlled to a single order of magnitude. This shows that the linear free-surface boundary conditions adequately describe the flow in this model.

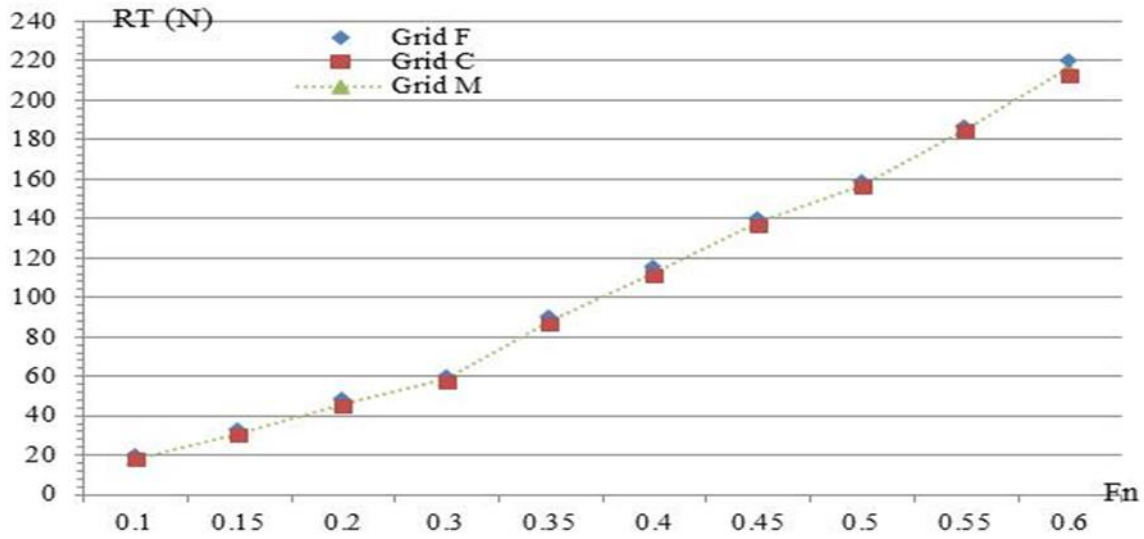

Fig. 16. Resistance curve for the submerged wing system (16 fins) using CFD

The comparison of results obtained from different mesh sizes indicated that the difference ε = (medium - coarse) / (fine - medium), where 0 < ε < 1 was slight and acceptable as presented in Table 4. The consistency of the numerical projections demonstrated how useful the overall numerical scheme was for predicting the resistance profile.

Table 4
The CFD results for the submerged system model

Fn	R_T (N) (Calculated)			$\varepsilon_{2.45\,m}$	Fn	R_T (N) (Calculated)			$\varepsilon_{2.45\,m}$
	Grid 1	Grid 2	Grid 3			Grid 1	Grid 2	Grid 3	
0.1	17.5	18.45	20.19	0.545977	0.4	110.65	113.18	115.78	0.973077
0.15	29.76	31.35	33.12	0.898305	0.45	136.22	138.12	140.15	0.935961
0.2	44.36	46.25	48.69	0.77459	0.5	155.62	157.39	159.24	0.956757
0.3	56.99	58.69	60.54	0.918919	0.55	184.69	185.32	187.12	0.35
0.35	86.25	88.24	90.32	0.956731	0.6	212.5	216.35	220.66	0.893271

The numerical predictions of the wing system were done to figure out a method for mesh generation under defined conditions to design the submerged glider system. The grid results were adequate and reasonable. The next step will validate the method by using the new fabricated model to be tested in the towing tank. Finally, the global view of the calculated wave patterns was evaluated, different planes for wave contours, wave contours (line) and contours of volume fraction (water) for the submerged wing system were presented in Figures 17 to 19.

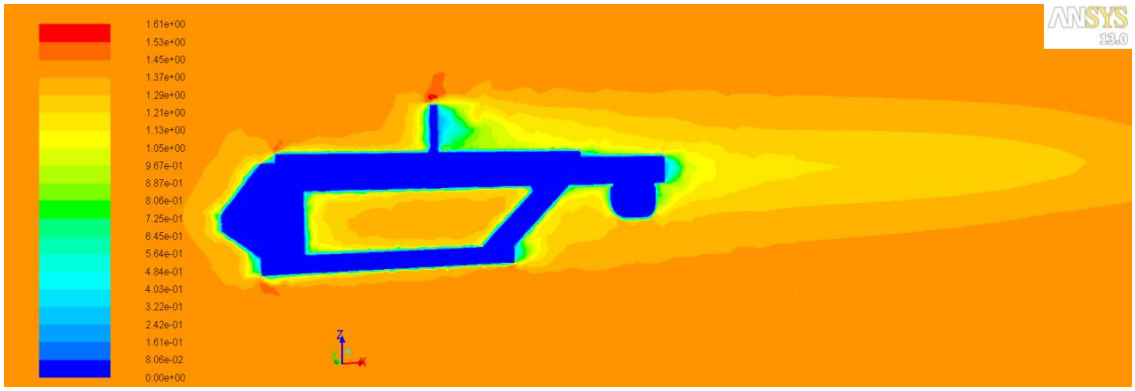

Fig. 17. Contours of velocity magnitude (mixture) and line for the model at Fn=0.40

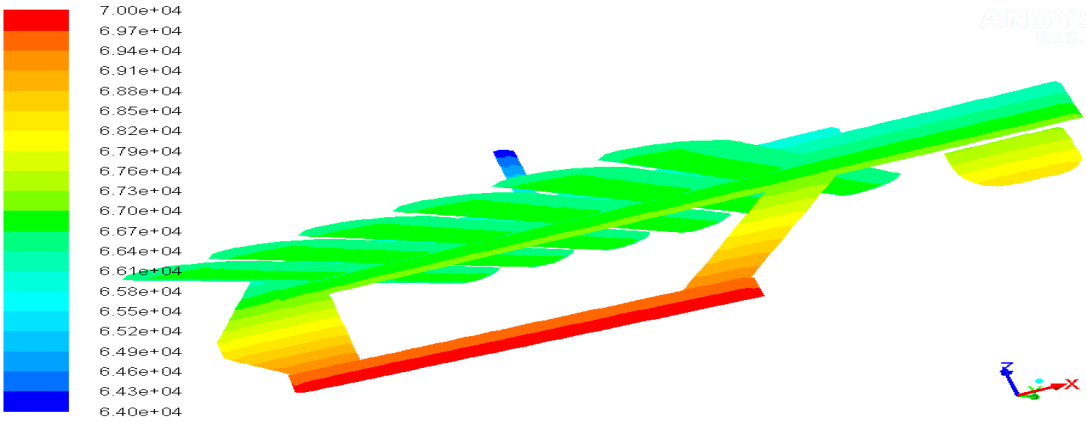

Fig. 18. Contours of static pressure for submerged glider system at Fn= 0.35

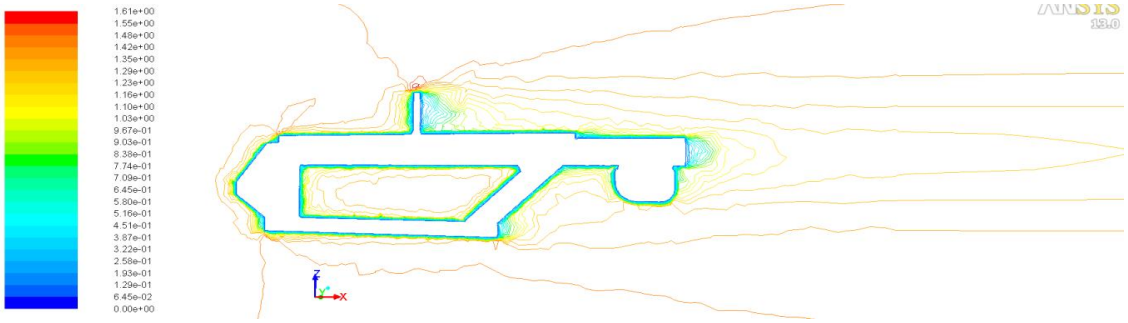

Fig. 19. Contours of velocity magnitude (line) for submerged wing system at Fn=0.40 and 0.32

7. Conclusion

This paper demonstrates investigation of the optimum hydrofoil wings used to design the submerged glider system from the resistance point of view. Flow around submerged wing system model has been calculated at different Froude numbers ranging from 0.1 to 0.6. The grid generator Gambit is used for meshing the computational domain with structured hexahedral and unstructured tetrahedral grid. Investigation for the computational efficiency of turbulence model is done. The numerical examination based on two-equation turbulence model for flow across NACA 0012 airfoil was carried out by using ANSYS Fluent at various AoA 15^{o} and at a Reynold number of 0.1 × 10^{6}. Crucial hydrodynamic point such as maximum lift and maximum efficiency AoA are determined. It is also concluded that VOF scheme with open channel boundary condition is effective in solving submerged flow problem. SST k-ω turbulence model predicts total resistance of the wing system more accurately.

The results obtained from the simulations are relatively limited and acceptable. Therefore, it can be concluded that the cambered plate and the hydrofoil NACA0012 can be practically applied in the design of the rudder and the wings of the model respectively from the resistance point of view. Furthermore, this investigation presents a new application for CFD calculation in estimating the resistance of the completely submerged glider system.

References

[1] Rozhdestvensky, Kirill. "Study of Underwater and Wave Gliders on the Basis of Simplified Mathematical Models." *Applied Sciences* 12, no. 7 (2022): 3465. https://doi.org/10.3390/app12073465

[2] M. P. C. (US); Roger G. Hine, P. V. C. (US); Derek L. Hine, L. A. C. (US); Joseph D. Rizzi, S. J. C. (US); Kurt A. F. Kiesow, A. A. (US); Robert Burcham, and S. J. C. (US) William A. Stutz, "WAVE POWER COMPONENTS, Patent NO.:US 8,287.323 B2," (2012).

[3] Ibrahim, M. D., S. N. A. Amran, A. Zulkharnain, and Y. Sunami. "Streamlined vessels for speedboats: Macro modifications of shark skin design applications." In *AIP Conference Proceedings*, vol. 1929, no. 1, p. 020023. AIP Publishing LLC, 2018. https://doi.org/10.1063/1.5021936

[4] Elhadad, Aladdin, Wen Yang Duan, and Rui Deng. "Comparative investigation of an automated oceanic wave surface glider robot influence on resistance prediction using CFD method." In *Applied Mechanics and Materials*, vol. 710, pp. 91-97. Trans Tech Publications Ltd, 2015. https://doi.org/10.4028/www.scientific.net/AMM.710.91

[5] Rochman, Refada Adyansya, Sayekti Wahyuningsih, Ari Handono Ramelan, and Qonita Awliya Hanif. "Preparation of nitrogen and sulphur Co-doped reduced graphene oxide (rGO-NS) using N and S heteroatom of thiourea." In *IOP Conference Series: Materials Science and Engineering*, vol. 509, no. 1, p. 012119. IOP Publishing, 2019. https://doi.org/10.1088/1757-899X/1052/1/012039

[6] Yusoff, Hamid, Koay Mei Hyie, Halim Ghaffar, Aliff Farhan Mohd Yamin, Muhammad Ridzwan Ramli, Wan Mazlina Wan Mohamed, and Siti Nur Amalina Mohd Halidi. "The Evolution of Induced Drag of Multi-Winglets for Aerodynamic Performance of NACA23015." *Journal of Advanced Research in Fluid Mechanics and Thermal Sciences* 93, no. 2 (2022): 100-110. https://doi.org/10.37934/arfmts.93.2.100110

[7] El Hady, Mohamed Adel. "A Comparative Study for Different Shapes of Airfoils." *Journal of Advanced Research in Fluid Mechanics and Thermal Sciences* 69, no. 1 (2020): 34-45. https://doi.org/10.37934/arfmts.69.1.3445

[8] Ng, Yu Han, Wah Yen Tey, Lit Ken Tan, Gerald Pacaba Arada, and M. W. Muhieldeen. "Numerical examination on two-equations turbulence models for flow across NACA 0012 airfoil with different angle of attack." *CFD Letters* 12, no. 2 (2020): 22-45.

[9] Chen, Xi, Mei Hong, Shiqi Wu, Kefeng Liu, and Kefeng Mao. "Design of Wave Glider Optimal Parameters Suitable for the Northwest Pacific Ocean, the North Indian Ocean, and the South China Sea." *Journal of Marine Science and Engineering* 9, no. 4 (2021): 408. https://doi.org/10.3390/jmse9040408

[10] Yang, Fuming, Weichao Shi, Xu Zhou, Bin Guo, and Dazheng Wang. "Numerical investigation of a wave glider in head seas." *Ocean engineering* 164 (2018): 127-138. https://doi.org/10.1016/j.oceaneng.2018.06.017

[11] J.-Y. Xie, W.-B. Xu, H. Zhang, P.-F. Xu, and W. Cui. "Dynamic modeling and investigation of maneuver characteristics of a deep-sea manned submarine vehicle." *China Ocean Eng* 23, no. 3 (2009): 505-516.

[12] Romadlon, Fajar, Dony Hidayat Al-Janan, Widya Aryadi, Rizqi Fitri Naryanto, Samsudin Anis, and Imam Sukoco. "Rotor Power Optimization of Horizontal Axis Wind Turbine from Variations in Airfoil Shape, Angle of Attack, and Wind Speed." *Journal of Advanced Research in Fluid Mechanics and Thermal Sciences* 94, no. 1 (2022): 138-151. https://doi.org/10.37934/arfmts.94.1.138151

[13] Merryisha, Samuel, and Parvathy Rajendran. "Experimental and CFD Analysis of Surface Modifiers on Aircraft Wing: A Review." *CFD Letters* 11, no. 10 (2019): 46-56.

[14] Yazik, Muhamad Hasfanizam Mat, Masaaki Tamagawa, Mohamed Thariq Hameed Sultan, and Adi Adzrif. "Computational study on aerodynamic characteristics and behaviour of S5010 airfoil." *Journal of Advanced Research in Fluid Mechanics and Thermal Sciences* 66, no. 1 (2020): 42-52.

[15] Abobaker, Mostafa, Sogair Addeep, Lukmon O. Afolabi, and Abdulhafid M. Elfaghi. "Effect of Mesh Type on Numerical Computation of Aerodynamic Coefficients of NACA 0012 Airfoil." *Journal of Advanced Research in Fluid Mechanics and Thermal Sciences* 87, no. 3 (2021): 31-39. https://doi.org/10.37934/arfmts.87.3.3139

[16] Ray, Sudipta, Dipankar Chatterjee, and Sambhunath Nandy. "Unsteady cfd simulation of 3d auv hull at different angles of attack." *Journal of Naval Architecture and Marine Engineering* 13, no. 2 (2016): 111-123. https://doi.org/10.3329/jname.v13i2.25849

[17] Ismail, Noor Iswadi, Mahamad Hisyam Mahamad Basri, Hazim Sharudin, Zurriati Mohd Ali, Ahmad Aliff Ahmad Shariffuddin, and Nik Muhammad Izwan Nik Mohd Kamel. "Investigations of Lift and Drag Performances on Neo-Ptero Micro UAV Models." *Journal of Advanced Research in Fluid Mechanics and Thermal Sciences* 84, no. 2 (2021): 50-62. https://doi.org/10.37934/arfmts.84.2.5062

[18] Deshpande, Sujay, P. Sundsbø, and Subhashis Das. "Ship resistance analysis using CFD simulations in Flow-3D." *The International Journal of Multiphysics* 14, no. 3 (2020): 227-236. https://doi.org/10.21152/1750-9548.14.3.227

[19] Elhadad, Aladdin, Wen Yang Duan, and Rui Deng. "A computational fluid dynamics method for resistance prediction of the floating hull of wave glider." In *Advanced Materials Research*, vol. 936, pp. 2114-2119. Trans Tech Publications Ltd, 2014. https://doi.org/10.4028/www.scientific.net/AMR.936.2114

[20] Husaini, Muhamad, Zahurin Samad, and Mohd Rizal Arshad. "CFD simulation of cooperative AUV motion." in *computer science*, (2009).

[21] Wu, Jianguo, Chaoying Chen, and Shuxin Wang. "Hydrodynamic effects of a shroud design for a hybrid-driven underwater glider." *Sea Technology* 51, no. 6 (2010): 45-47.

[22] Rosemurgy, William J., Deborah O. Edmund, Kevin J. Maki, and Robert F. Beck. "A Method for resistance prediction in the design environment." In *11th International Conference on Fast Sea Transportation FAST*. 2011.

[23] Menter, Florian R. "Two-equation eddy-viscosity turbulence models for engineering applications." *AIAA journal* 32, no. 8 (1994): 1598-1605. https://doi.org/10.2514/3.12149

[24] Bao, Han, and Haitao Zhu. "Modeling and trajectory tracking model predictive control novel method of AUV based on CFD data." *Sensors* 22, no. 11 (2022): 4234. https://doi.org/10.3390/s22114234

[25] Ferziger, Joel H., Milovan Perić, Robert L. Street, Joel H. Ferziger, Milovan Perić, and Robert L. Street. "Solution of the Navier–Stokes Equations: Part 1." *Computational Methods for Fluid Dynamics* (2020): 183-226. https://doi.org/10.1007/978-3-319-99693-6_7